Heliyon 8 (2022) e10167

Contents lists available at ScienceDirect

Heliyon

journal homepage: www.cell.com/heliyon

Research article

Preparation and characterization of rice husk activated carbon-supported zinc oxide nanocomposite (RHAC-ZnO-NC)

Adewumi O. Dada [a,c,e,f,g,*], Adejumoke A. Inyinbor [a,e,f], Blessing E. Tokula [a,e,f,*], Olugbenga S. Bello [b,e,f], Ujjwal Pal [c,d]

[a] Industrial Chemistry Programme, Nanotechnology Laboratory, Department of Physical Sciences, Landmark University, P.M.B.1001, Omu-Aran, Kwara, Nigeria
[b] Department of Pure and Applied Chemistry, Ladoke Akintola University of Technology, Ogbomoso, Nigeria
[c] Department of Energy and Environmental Engineering, CSIR-Indian Institute of Chemical Technology, Hyderabad, India
[d] Academy of Scientific and Innovative Research (AcSIR), Ghaziabad 201002, India
[e] Landmark University SDG 6 (Clean Water and Sanitation), Nigeria
[f] Landmark University SDG 11 (Sustainable Cities and Communities), Nigeria
[g] Landmark University SDG 12 (Responsible Consumption and Production), Nigeria

ARTICLE INFO

Keywords:
Zinc oxide
Nanocomposites
Rice husk
Activated carbon
Characterization

ABSTRACT

Indiscriminate waste discharge into water bodies has increased the level of water pollution via anthropogenic activities. Hence the need for the development of sustainable and environmentally benign nanomaterials has the potential for wastewater treatment. Rice husk activated carbon (RHAC) prepared by orthophosphoric acid activation was successfully loaded with freshly prepared ZnO nanoparticles by a bottom-up approach via precipitation method resulting in the RHAC-ZnO-NC. RHAC-ZnO-NC's mineralogy with 72% zincite was determined by XRD, morphology by SEM, and the functional group by FTIR. The physicochemical parameters showed surface area 615.2 $m^2\ g^{-1}$, pH (pzc) (6.62), pH (6.53), bulk density (0.88 g/cm^3), ash content (18.45%), and volatile matter (58.08%). The porosity was determined by iodine number. Boehm titration was carried out for oxygen-bearing functional group determination. The study substantiated RHAC-ZnO-NC as a promising material for adsorption and photocatalytic degradation.

1. Introduction

The increase in the global population has led to an increase in food demand. Agricultural waste is therefore inevitable in Nigeria as farming practices are greatly on the increase. They are by-products of agricultural practices regarded as agro-residues such as rice husk, plantain peel, coconut husk, sugarcane bagasse, groundnut shell, etc. These agro-wastes are mostly discarded indiscriminately into streams and rivers, and incinerated thus, leading to various environmental problems [1]. The rice husk is the covering obtained after the milling process is carried out on the rice grain. The husk is the outermost covering on the rice grain and makes us 20–25% of the grains' total weight. After the milling, disposal of the husk becomes a major challenge in many areas and as such end up being burnt or discarded indiscriminately, causing lots of environmental pollution. Researchers have therefore shown keen interest in the conversion of rice husk targeting the production of activated carbon for remediation, therefore, serving as a technique for waste management [2, 3]. In recent times, agro-waste valorization has been on the increase. Numerous advantages exist for the use of such agro-waste-based activated carbon ranging from the high removal efficiency to its cost-effectiveness and ease of modification. Thus, low-value wastes are converted to high-value adsorbents [4]. The low selectivity serves as a huge limitation to the broad utilization of activated carbon for the removal of pollutants. As such, various techniques have been employed by researchers to modify and increase the adsorption capacity, porosity, and surface area of activated carbon [5]. Loading activated carbon with nanoparticles has attracted a lot of attention as a means of modification because nano-composites combine the individual properties of the nanoparticles and activated carbon leading to an adsorbent with enhanced adsorptive capacity. Among the types of nanoparticles, metal oxides vis-à-vis core-shell zerovalent iron, manganese oxide, zinc oxide, titanium oxide, copper oxide and cesium oxide have been reported as operational adsorbents for pollutants' removal owing to their uniqueness in terms of surface area, selectivity, and ability to penetrate the contamination zone of pollutants [6, 7, 8, 9]. They possess large areas as matrices or stabilizers to obtain hybrid

* Corresponding authors.
E-mail addresses: dada.oluwasogo@lmu.edu.ng (A.O. Dada), tokula.blessing@lmu.edu.ng (B.E. Tokula).

https://doi.org/10.1016/j.heliyon.2022.e10167
Received 12 October 2021; Received in revised form 22 March 2022; Accepted 28 July 2022

nano-composite adsorbents. These nanocomposites have shown the capacity to increase the sorption capacity of the adsorbents to which it is loaded. Nano-composites have exhibited efficiency in the sorption of various pollutants such as pharmaceuticals [27] dyes [25, 26, 29], and heavy metals [25]. Equally, these nanocomposites have been shown to have reusability capacity without a drastic or ridiculous reduction in the efficiency of the adsorbent [9]. Thus, this study aims at preparing and characterizing rice husk-activated carbon-supported zinc oxide nanocomposite (RHAC-ZnO-NC).

2. Materials and method

2.1. Sample collection and preparation

Rice husk was obtained from Landmark University Research Farm, Kwara State, Nigeria with a location (of 8.1239° N, 5.0834° E, Omu Aran). It was screened and thoroughly washed to remove impurities and dust. Using distilled water, the rice husk was then rinsed and oven-dried for 3 h at 110 °C. The rice husk (30 g) was then treated with 100 mL nitric acid (1.0 M HNO_3) with a pretreatment ratio of 1:2 to remove metallic impurities, rinsed and dried, and then treated with 1.0 M NaOH to remove silica content and brick red coloured RH was obtained. Then, it was transferred to a furnace for carbonization at 400 °C for 1 h.

2.2. Carbonization and chemical activation

The temperature required for carbonization must be carefully selected to ensure that the sample does not turn to ash. The temperature must however be sufficient to carbonize all existing non-carbon compounds and increase the pore spaces and surface area of the adsorbent. 500 g of the treated RH was measured into 1000 mL beaker containing 1 M H_3PO_4. The beaker content was heated for about 10 h at 70 °C till a paste was formed. The paste in the crucible was heated at 400 °C in a muffle furnace for 1 h at a heating rate of 5 °C per min to enhance pore opening. The resulting RHAC was cooled and later thoroughly rinsed with DI to obtain a neutral pH. The pore opening leading to a large surface area was synergistically enhanced by both the carbonization and chemical activation [2, 10]. The activated carbon was oven-dried at 105 °C, labelled RHAC and thereafter kept in a desiccator (air-tight) for further utilization.

2.3. Nano-composite synthesis

The synthesis of ZnO nanocomposites was carried out by slight modification to the method as described in our previous studies [7, 11, 12, 13, 14]. 1.5 M $(NH_4)_2CO_3$ solution was stirred vigorously with 5 g as-prepared RHAC. 1.0 M Zn $(NO_3)_2$ solution was then slowly added to it. A white precipitate was formed on the activated carbon, the nanoparticles began to form immediately within 2 min like a white colloidal precipitate turning grey as a result of a homogeneous mixture with black as-prepared RHAC. The reaction was allowed to age for 3 h while grey particles paste formed in 3 h. The loaded RHAC-ZnO-NC a filtered using Whatman filter paper and rinsed repeatedly with water and ethanol. The rinsed nanocomposite was dried in a hot-air oven at 110 °C for 6 h, thereafter annealed, ground, and calcined in a furnace for 4 h at 550 °C. After cooling, it was stored in an airtight container labelled as RHAC-ZnO-NC.

2.4. pH determination

1.0 g of the nano-adsorbent (RHAC-ZnO-NC) was weighed and placed into a beaker. 100 mL of distilled water was added and allowed to boil for 5 min. Afterwards, the solution was diluted to 200 mL, allowed to cool and obtained pH value was recorded.

2.5. pH point of zero-charge (pH_{pzc}) determination

The pH (pzc) was determined by adding 0.1 g of RHAC-ZnO-NC into a 250 mL conical flask containing 50 mL of 0.1 M NaCl. This was done differently in ten (10) conical flasks while the pH of each flask was varied from pH 2 to 12 using 0.1 M NaOH or HCl. Thereafter, it was sealed and shaken for 24 h. The final pH was determined and a plot of the difference between the final and initial pH, ($pH_f - pH_i$) against the initial pH was plotted. The pH (pzc) was observed as the point where the plotted line cuts the x-axis (initial pH axis) which is when the final pH equals zero [15].

2.6. Bulk density determination

The determination of the bulk density was carried out using the method described in the literature [30]. A 10 mL measuring cylinder was weighed after and before it was packed with water. The RHAC-ZnO-NC sample was then packed into the measuring cylinder, tapped 2–3 times, and then re-weighed. The difference in weight was determined and the bulk density was determined with Eq. (1):

$$Bulk\ density = \frac{W_2 - W_1}{v} \quad (1)$$

Where:

W_2 = Weight of cylinder filled with sample.
W_1 = Weight of empty measuring cylinder.
V = Volume of cylinder.

2.7. Moisture content

This was evaluated following the method as described in the literature [4, 16]. The empty crucible was weighed and 1.0 g of the RHAC-ZnO-NC was weighed into it after which it was placed in an oven and heated for 5 h at 110 °C in an oven. The cooled sample placed in a desiccator was reweighed. The moisture content was obtained by weight difference divided by initial weight using Eq. (2):

$$Moisture\ \% = \frac{loss\ in\ weight\ on\ drying\ (g)}{initial\ weight\ (g)} \times 100 \quad (2)$$

2.8. Ash content

The ash content was determined using the method described by Ref. [17]. The crucibles were first preheated, cooled in a desiccator and weighed. 1.0 g of RHAC-ZnO-NC was measured into the crucibles and transferred to the furnace, thereafter allowed to heat at 500 °C for about 1 h 30 min. This was placed in a desiccator for cooling and the final weight was measured. Eq. (3) was used to calculate the % Ash content

$$\%Ash = \frac{ash\ \ weight}{oven\ \ dry\ \ weight} \times 100 \quad (3)$$

2.9. Volatile matter

The volatile matter determination of RHAC-ZnO-NC was carried out by weighing the empty crucible and then placing 1.0 g of the sample. The sample placed in a furnace was allowed to rise to 500 °C. At 500 °C, the sample was heated for 10 min, and thereafter cooled before the final weight was measured. The value of the % volatile matter was calculated using Eq. (4) [17]:

$$\%\ Volatile\ \ matter = \frac{weight\ \ of\ \ volatile\ \ component\ \ (g)}{oven\ \ dry\ \ weight\ \ (g)} \times 100 \quad (4)$$

2.10. Surface area determination by Sears methods

The adsorbent surface area was determined using Sear's method. 0.5 g of as-prepared RHAC-ZnO-NC was measured into a 250 mL conical flask having 50 mL of 1 g NaCl. The mixture's pH was raised using 0.1 M HCl to pH 3–3.5. Titration was done with 0.1 M NaOH to raise the pH to 4 and

Table 1. Physicochemical characteristics of RHAC-ZnO nanocomposites.

Property	RHAC-ZnO nanocomposite
Surface area (sears method)	615.2 $m^2\ g^{-1}$
% Moisture content	17.72
Bulk density	0.88
Ash content (%)	18.45
Volatile matter (%)	58.007
pH_{pzc}	5.10
pH	6.53

then raised to 9. The difference in the volume required to raise the pH from 4 to 9 was recorded and utilized to evaluate the surface area using Eq. (5) [11, 14, 18, 19]:

$$S\ (m^2 / g) = 32V - 25 \tag{5}$$

2.11. Iodine number determination

Iodine number for pore determination was carried out following the method described in the literature [20]. A 1000 mL stock solution comprising 2.7 g iodine pellets and 4.1 g KI (potassium Iodide) was prepared. This was standardized using sodium thiosulphate (standard solution). In a 100 mL flask, 10 mL of 5% v/v HCl together with 0.5 g RHAC-ZnO-NC was added with constant stirring to wet the sample. 100 mL of the prepared stock iodine solution was placed on the shaker for 60 min after which it was filtered. 0.1 M sodium thiosulphate was placed in a burette and titrated with 20 mL of the filtered RHAC-ZnO-NC solution. The amount of iodine adsorbed was calculated using Eq. (6)

$$\frac{Img}{g} = \frac{B - S}{B} \times \frac{VM}{W} \times 253.81 \tag{6}$$

Where W represents the adsorbents mass, B and S represents the volumes of thiosulphate solution required for blank and sample titrations, respectively, 253.81 is the atomic mass of iodine and V is the 20 mL aliquot while M is the concentration of the iodine solute.

Comparison of the porosity and surface area of both the base material, RHAC and the nanocomposite, RHAC-ZnO-NC, from this study could be estimated using Eqs. (7) and (8) [21]:

$$Iodine\ value = \frac{Concentration \times atomic\ mass \times normality \times volume\ of\ iodine}{Mass\ of\ activated\ carbon \times volume\ of\ blank\ thiosulphate} \tag{7}$$

$$S_{BET} = \frac{Iodine\ value \times 10^{-3}}{Atomic\ mass\ of\ Iodine} \times N_A \times \omega \tag{8}$$

Where N_A = Avogadro's number = 6.023×10^{23} and $\omega = 0.2096 \times 10^{-18}$.

2.12. Fourier transform infrared (FTIR) analysis

The various functional groups were determined by FTIR analysis using an FTIR spectrometer (PerkinElmer FTIR-2000).

2.13. Determination of oxygen containing functional groups by Boehm method

The Boehm titration method as described by Bello et al (2017) [14] was adopted for this analysis. One gram of RHAC-ZnO-NC was placed in a beaker having 15 mL of 0.1 M NaOH, 0.5 M Na_2CO_3 and $NaHCO_3$ (0.1 M) solutions for groups that are acidic. However, for basic groups, 0.1 M HCl solution was used and at ambient temperature, for 48 h they were placed on a shaker. The solution was back titrated with NaOH (0.1 M) for basic groups and HCl (0.1 M) for acidic groups. Due to the ability of NaOH to neutralize phenolic, lactonic and carboxylic groups and Na_2CO_3 to neutralize carboxylic and lactonic groups and $NaHCO_3$ to neutralize carboxylic groups only, the number of oxygen-containing functional groups can be evaluated using Eq. (9):

$$F_X = \frac{V_{bx} - V_{ex}}{M_X} \times M_t \times D_F \tag{9}$$

Where V_{bx} is the volume of titrant used to titrate the blank, D_F is the dilution factor, F_x ($mmolg^{-1}$) is the amount of oxygen-containing functional groups, M_t is the molarity of the titrant used, V_{ex} is the volume of the titrant used to titrate the extract [22].

2.14. Electron microscopy (SEM) analysis

Scanning Electron Microscopy (SEM) is a technique based on electron-material interactions, capable of producing images of the sample surface.

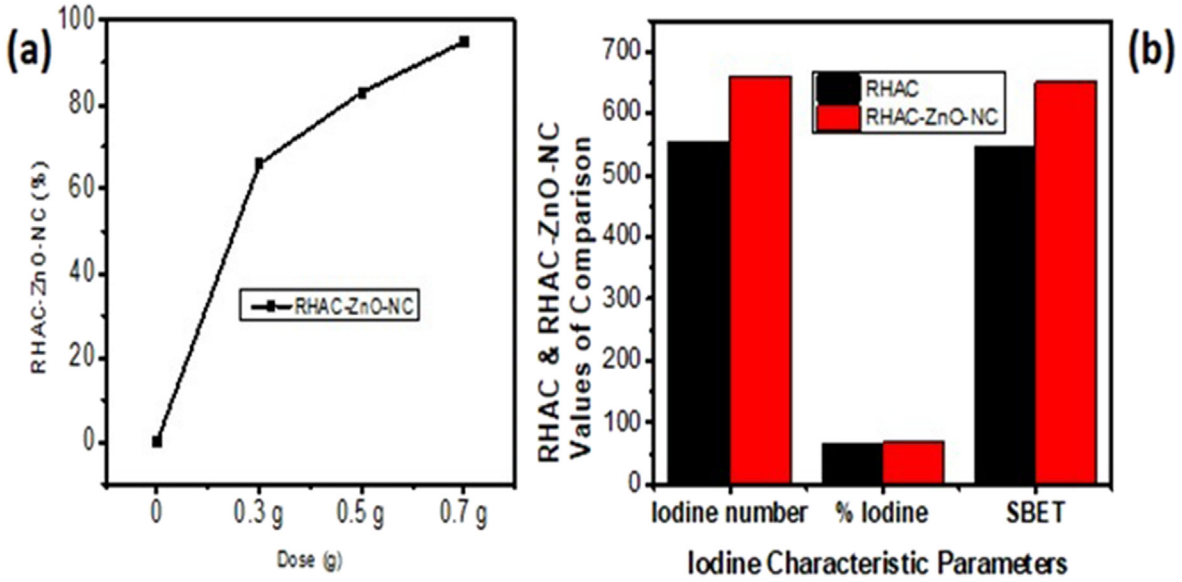

Figure 1. (a) Surface porosity determination by iodine adsorption (b) iodine characteristic parameters.

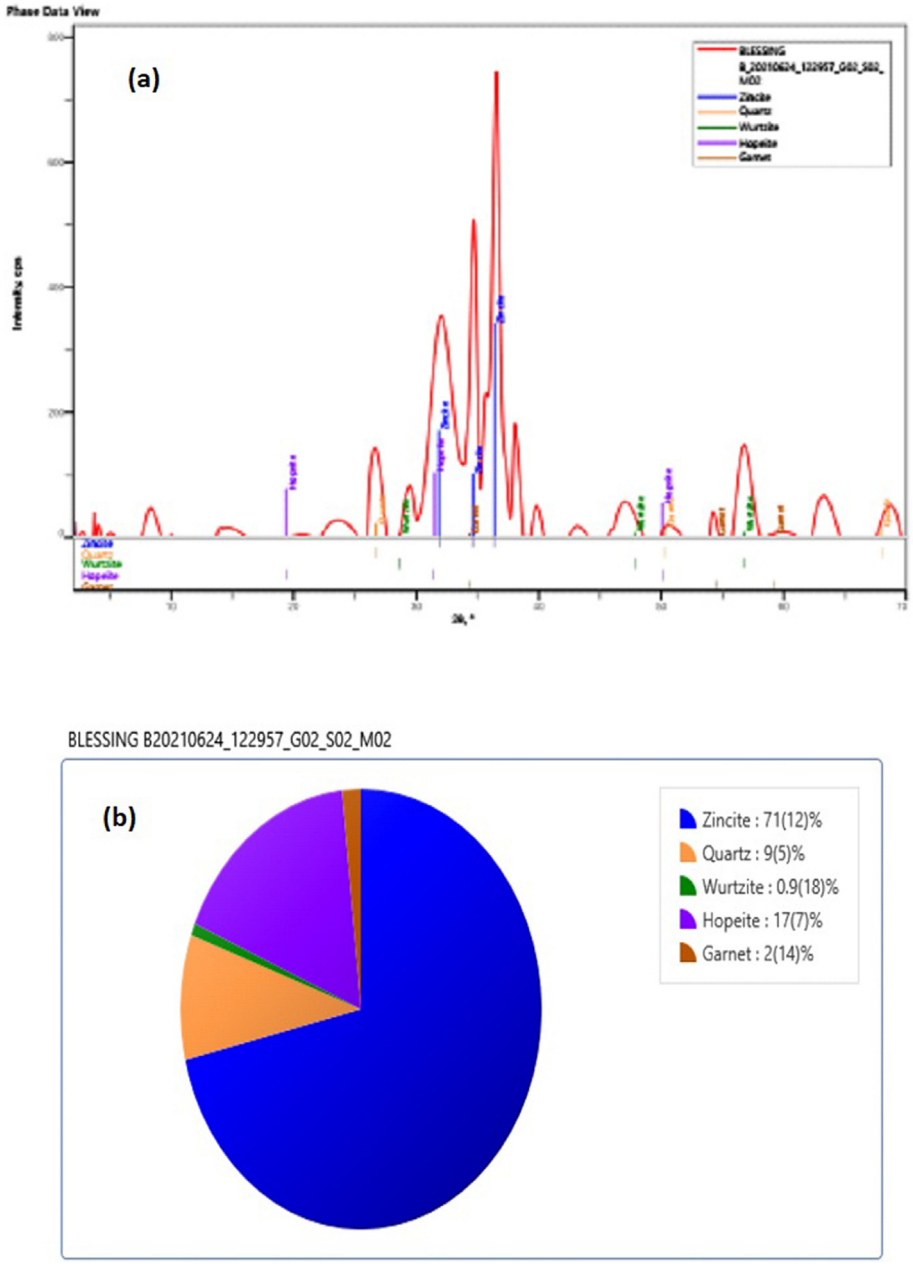

Figure 2. (a) XRD analysis and (b) elemental distribution of RHAC-ZnO nanocomposites.

These particles are analyzed by various detectors which give a three dimensions image of the surface. This technique was used to study the morphological feature and surface characteristics of the prepared adsorbents [22].

2.15. X-ray diffraction (XRD) analysis

The X-ray Diffraction Schmaltz model XRD 6000 automated with Ni-Filtered Cu Kα radiation was used to investigate the material structure of RHAC-ZnO nanocomposites.

3. Results and discussion

The loading of nanoparticles onto activated carbon improved the physicochemical properties, surface morphology, oxygen groups, and crystallinity of the resultant nano-composite.

3.1. Moisture content, ash content, volatile matter, and bulk density physicochemical characterization of RHAC-ZnO-NC

The physicochemical characteristics of the RHAC-ZnO-NC are presented in Table 1. Results reveal low ash, moisture, and volatile matter content. High moisture content dilutes the capacity of carbon thereby causing additional weight [23]. Lower moisture content is desirable for the material to be applied for remediation such as RHAC-ZnO-NC. From this study as seen in Table 1, the moisture content obtained for RHAC-ZnO-NC being 17.2%, is in an acceptable range when compared to other materials containing activated carbon as obtained in other studies. It is lower than the one obtained by Leena *et al.* (2015) [24], and that reported by Ekpete for Fluted Activated Carbon (FAC) (19.50%) [25].

Ash content influences the ignition point of carbon leading to a reduction of its capacity when used for remediation. This implies that the efficiency of RHAC-ZnO-NC could be affected by the ash content

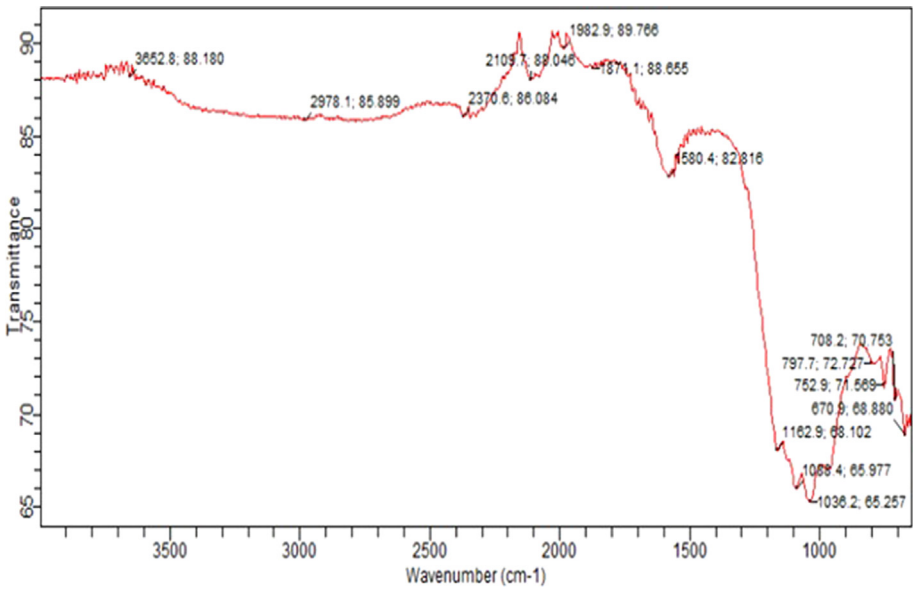

Figure 3. FTIR spectrum of RHAC-ZnO nanocomposites.

therefore composite of activated carbon with lower ash content is more preferred. 18.45% ash content is obtained in this study as presented in Table 1. A range of 1–20% is reported to be the acceptable range for ash content [26, 27]. The value obtained for volatile matter content was lower than those reported by [28] on rice husk activated carbon which indicates an improvement over the activated carbon due to the doping by ZnO leading to the formation of RHAC-ZnO-NC.

The bulk density is also an important parameter as it gives the degree of filterability and equilibration of the adsorbent. Presented in Table 1 is the bulk density of RHAC-ZnO-NC which was observed as 0.88 ± 0.02 g cm^{-3}. This implies better equilibration which is expected for nano-materials or developed adsorbents. In this study, the bulk density being less than 1.2 g cm^{-3} is an indication that RHAC-ZnO-NC would be a suitable nanocomposite for remediation or photocatalytic studies. This observation is supported by Moyo *et al.*, 2013 [23].

3.2. The isoelectric point determination via pH and pH_{pzc}

The pH was found to be 6.53 and the pH_{pzc} at 5.10 as shown in Table 1. This was in agreement with reports on the pH of 6–8 as acceptable limits for applications [17]. Since, the values of pH > pH_{pzc}, the surface charge on the RHAC-ZnO-NC is negative which would give it relevance in the adsorption of cationic pollutants. More so, nanocomposite or its activated carbon hybrid have been reported effective at lower pH within the acceptable range 6–8 [28].

3.3. Iodine number

One of the most fundamental parameters to measure carbon performance is the iodine number. Since the base material used in the formation of RHAC-ZnO-NC contains, carbon content, the determination of iodine number parameters becomes imperative. Iodine number is also regarded as the measure of the carbon content by adsorption of iodine molecule. Advantageously, it could be applied in determining the porosity and the total surface area which are relevant physicochemical parameters in support of other methods of surface area determination. Therefore, to determine the carbon performance as a base material used in RHAC-ZnO nanocomposite for this study, to measure porosity, as well as surface area, iodine adsorption studies, become imperative. Figure 1a depicts the porosity determination by iodine adsorption at different RHAC-ZnO dosages. The result shows that the percentage of iodine adsorbed increases from 66 to 95 as the RHAC-ZnO-NC dosage also increases due to an increase in porosity as a measure of an increase in the active sites [26]. A similar observation was reported in adsorption studies where the effect of adsorbent dosage was investigated [7, 30]. Figure 1b shows the comparison of the rice husk activated carbon (RHAC) base material and RHAC-ZnO-NC nanocomposite. The Iodine number of RHAC-ZnO-NC (660.4), average % Iodine (68%) and S_{BET} (651.15 m^2 g^{-1}) surpassed that of RHAC (base material) and several other materials reported in the literature such as commercial activated carbon (200.36) [20], moringa leaf raw (MLR = 92.24), moringa leaf acid and base activated, 182.29 and 169.18 respectively [29], and ground pine activated carbon (GPAC) 483.5 [31]. Further confirmation of the high surface area of RHAC-ZnO-NC is the specific surface area determined and presented in Table 1. The higher iodine parameters (Figure 1b) of RHAC-ZnO-NC further signposted it as better nano adsorbents that could find relevance in wastewater remediation and a cleaner environment.

Table 2. Oxygen containing functional groups.

Groups	RHAC-ZnO nanocomposite
Carboxylic (meq/g)	0.09
Phenols (meq/g)	0.12
Lactones (meq/g)	0.03
Basic sites (meq/g)	0.21

Table 3. Vibrational band assignment of peaks for FTIR spectrum of RHAC-ZnO nanocomposites.

Wave number	Vibrational band assignment
3652.8	O–H stretch
2978.1	C–H aliphatic stretch
2370.6	C=N stretch
2109.7	C≡C stretch
1982.9	C=O symmetric stretch
1871.1	C=O stretch of carboxylic acid/acid halide
1580.4	C=C stretch
162.9	C–O stretch
1036.2	C–O stretch
797.7	=C–H bend
670.9	ZnO

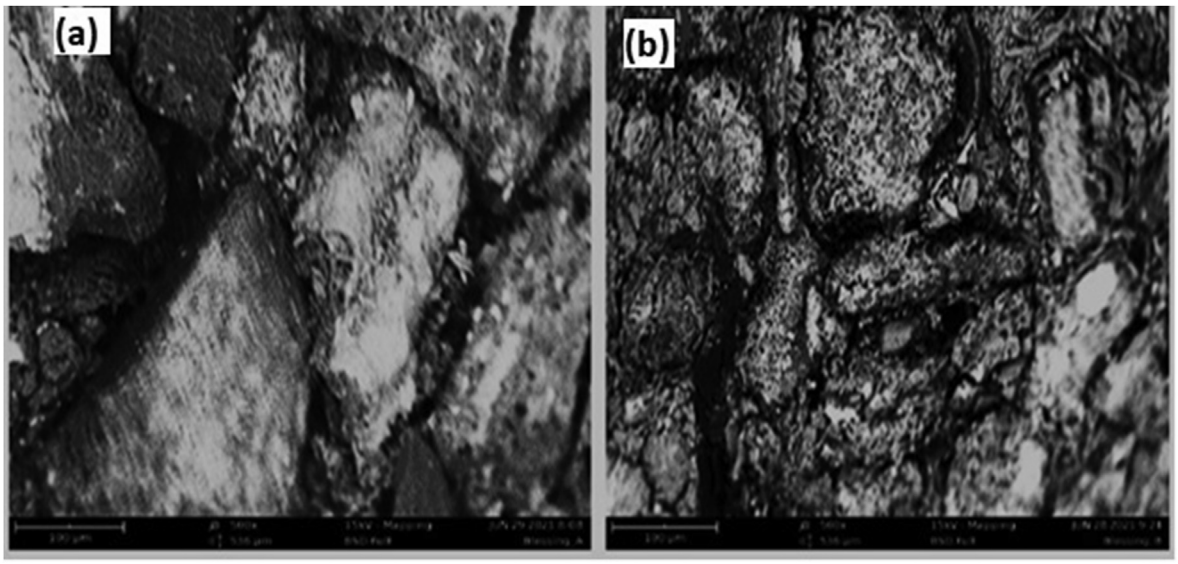

Figure 4. SEM images of (a) RHAC and (b) RHAC-ZnO nanocomposites.

3.4. XRD analysis of RHAC@ZnO

Figure 2(a&b) show the XRD pattern and the elemental distribution of RHAC-ZnO nanocomposite. Figure 2a depicts the crystallinity nature of RHAC-ZnO as evidence of ZnO formation in the loading of RHAC-ZnO. The XRD pattern displayed in Figure 2a measured at 2 theta was from 1 – 70°. The values of the peaks at 29.9°, 48° and 57° correspond to wurtzite. Prominent peaks at 32°, 34°, 36°, 37° also correspond to zincite [32]. Other peaks at 48°, 52°, 55°, 62°, 65°, and 68° correspond to quartz, hopetite, and granet with their corresponding percentage distribution as displayed in Figure 2b. The constituents from Figure 2a&b confirm RHAC-ZnO as nanocomposite. Notable characteristic peaks from the XRD pattern observed in Figure 2a confirmed the presence of ZnO when compared with the JCPDS card no 36-1451. This observation is supported by the report of Prabhu *et al.*, 2019 [33] and Uma *et al.*, 2019 [34].

3.5. Surface chemistry by functional group determination

Figure 3 presents the FTIR spectrum of RHAC-ZnO nanocomposite. Some of the various band assignments are presented in Table 2. The weak bands between 3652 and 3317 correspond to a hydroxyl group (–OH) of intramolecular bonds [35], 2978 cm^{-1} ascribed to C–H stretch of aliphatic, 2370.6 cm^{-1} assigned to C=N stretch, 1848 cm^{-1} is assigned to –C=O stretch of carboxylic acid or an acid halide, a signal at 1595 cm^{-1} is –C=C– of alkene [36]. Other vibrational bands are presented in Table 3. More of the oxygen-bearing functional group contains an acidic site as can be confirmed from the Boehm analysis. The shift in the band of ZnO to 670.9 cm^{-1} could be due to the doping of the RHAC. Mainly the bands between 1580 cm^{-1} and 1036 cm^{-1} are assigned to ring vibration in aromatic mostly common to carbonaceous materials [37].

3.6. The Boehm titration

This gives information on the concentration and type of functional groups of RHAC-ZnO-NC. As shown in Table 2, the acidic group of the oxygen-containing functional groups are carboxylic (0.09 meq/g), phenols (0.12 meq/g), and lactones (0.03 meq/g) cumulating to a total of 0.24 mmol/g while the basic group is 0.21 mmol/g. The number of basic groups is much lower in comparison to acidic groups suggesting that there are more oxygen-bearing functional groups as depicted in Table 2 hence more acidic sites. This is also supported by the pH point of zero charges found to occur at 5.10 depicting a positive charge in solution up to pH(pzc) = 5.10 above this pH, the surface of RHAC-ZnO-NC would be negative. This further supported the dominance of the acid sites in the oxygen-bearing functional group found in FTIR analysis. This finding is supported by the report of Nethaji *et al.* (2013) [38] and Bello *et al.* (2014) [39].

3.7. Scanning electron microscopy (SEM) analysis of RHAC-ZnO-NC

Figure 4(a&b) show the SEM micrographs of pure rice husk activated carbon (RHAC) (Figure 4a) and RHAC-ZnO-NC (Figure 4b). Shown in Figure 4a are trapezoidal and porous surfaces which were improved upon when RHAC-ZnO-NC was formed. This reveals irregular, rough, coarse surfaces with different cracks and crevices which reveal the existence of well-developed pores [36, 37, 40, 41, 42]. It is suggested that these pores could have resulted from the physical and chemical activation as well as the doping with ZnO resulting in the formation of RHAC-ZnO-NC. These developed pores could serve as the site for swallowing and trapping pollutant molecules when RHAC-ZnO-NC is applied for adsorption and remediation. More so, the pores could also enhance the uninterrupted flow of adsorbate.

4. Conclusion

Preparation and characterization of RHAC-ZnO-NC were the main aims of this study. By controlled precipitation, RHAC-ZnO-NC was successfully prepared. From the physicochemical characterization, the moisture content (17.2%), ash content (18.4%), and bulk density (0.88 g cm^{-3}) suggested the development of unique characteristics of RHAC-ZnO-NC over its base material, RHAC which is pure activated carbon. The pH > pH(pzc) (6.63 > 5.10) depicts a negative surface that could be suitable for cationic pollutant degradation or remediation. RHAC-ZnO possesses a high specific surface area (615 $m^{2\ g\text{-}1}$), Iodine number (660.4), average % Iodine (68%) and S_{BET} (651.15 $m^{2\ g\text{-}1}$). XRD pattern showed the crystallinity structure of RHAC-ZnO-NC with characteristic peaks corresponding to wurtzite and zincite confirming the presence of ZnO. Other elemental constituents show the presence of quartz, hopetite, and granet. The functional group from the surface chemistry study was revealed by FTIR which was supported and affirmed by the presence of oxygen-bearing functional groups, a more acidic site than the basic site as determined by Boehm analysis. SEM analysis revealed the presence of irregular, rough, coarse surfaces with different cracks and crevices which reveal the existence of well-developed pores. This study opined and revealed that RHAC-ZnO-NC is a promising nanocomposite that would find relevance in environmental remediation and industrial wastewater treatment.

Declarations

Author contribution statement

Adewumi O. Dada: Conceived and designed the experiments; Performed the experiments; Analyzed and interpreted the data; Contributed reagents, materials, analysis tools or data; Wrote the paper.

Adejumoke A. Inyinbor: Conceived and designed the experiments; Analyzed and interpreted the data; Contributed reagents, materials, analysis tools or data.

Blessing E. Tokula: Performed the experiments; Analyzed and interpreted the data; Contributed reagents, materials, analysis tools or data; Wrote the paper.

Olugbenga S. Bello, Ujjwal Pal: Analyzed and interpreted the data; Contributed reagents, materials, analysis tools or data.

Funding statement

This research did not receive any specific grant from funding agencies in the public, commercial, or not-for-profit sectors.

Data availability statement

Data will be made available on request.

Declaration of interests statement

The authors declare no conflict of interest.

Additional information

No additional information is available for this paper.

Acknowledgements

The authors' appreciated the Management of Landmark University for the provision of a research-enabling environment and facilities. The authors are grateful to the Faculty and staff of the Industrial Chemistry Programme and Nanotechnology laboratory, Landmark University, for their assistance. The concept, exposure, and drive provided by leaders of research groups on this paper are equally appreciated.

References

[1] V.D. Rajput, C. Yaning, Biosorption of heavy metals using agrowaste: a review, Pollut. Res. Pap. 34 (1) (2015) 34–38.
[2] A.O. Dada, J.O. Ojediran, A.P. Olalekan, Sorption of Pb^{2+} from aqueous solution unto modified rice husk: isotherms studies, Adv. Phys. Chem. 2013 (2013) 1–7, 842425.
[3] B. Orimolade, F. Adekola, M.A. Aminat, Removal of bisphenol-A from aqueous solution using rice husk nanosilica: adsorption kinetics, Equilib. Thermodyn. Stud. 12 (3) (2018) 8–221.
[4] J.O. Ojediran, A.O. Dada, S.O. Aniyi, R.O. David, Functionalized Zea Mays Cob (FZMC) as low-cost agro-waste for effective adsorption of malachite green dyes data set, Chem. Data Collect. 30 (2020), 100563.
[5] E. Alipanahpour, M. Ghaedi, A. Asfaram, F. Mehrabi, Efficient adsorption of Azure B onto CNTs/Zn: ZnO@Ni2P-NCs from aqueous solution in the presence of ultrasound wave based on multivariate optimization, J. Ind. Eng. Chem. 74 (2019) 55–62.
[6] B.R. White, B.T. Stackhouse, J.A. Holcombe, Magnetic γ-Fe2O3 nanoparticles coated with poly-l-cysteine for chelation of As(III), Cu(II), Cd(II), Ni(II), Pb(II) and Zn(II), J. Hazard Mater. 161 (2009) 848–853.
[7] A.O. Dada, F.A. Adekola, E.O. Odebunmi, Liquid phase scavenging of Cd (II) and Cu (II) ions onto novel nanoscale zerovalent manganese (nZVMn): equilibrium, kinetic and thermodynamic studies, Environ. Nanotechnol. Monit. Manag. 8 (2017) 63–72.
[8] C. Tamez, R. Hernandez, J.G. Parsons, Removal of Cu (II) and Pb (II) from aqueous solution using engineered iron oxide nanoparticles, Microchem. J. 125 (2016) 97–104.
[9] N. Masoudian, M. Rajabi, M. Ghaedi, Titanium oxide nanoparticles loaded onto activated carbon prepared from bio-waste watermelon rind for the efficient ultrasonic-assisted adsorption of Congo red and phenol red dyes from wastewaters, Polyhedron 173 (2019), 114105.
[10] A.A. Spagnoli, D.A. Giannakoudakis, S. Bashkova, Adsorption of methylene blue on cashew nut shell based carbons activated with zinc chloride: the role of surface and structural parameters, J. Mol. Liq. 229 (2017) 465–471.
[11] A.O. Dada, A.A. Inyinbor, O.S. Bello, B.E. Tokula, Novel plantain peel activated carbon–supported zinc oxide nanocomposites (PPAC-ZnO-NC) for adsorption of chloroquine synthetic pharmaceutical used for COVID-19 treatment, Biomass Convers. Biorefinery 1 (2021) 3.
[12] K.S. Obayomi, A.E. Oluwadiya, S.Y. Lau, A.O. Dada, D. Akubuo-Casmir, T.A. Adelani-Akande, A.S.M. Fazle Bari, S.O. Temidayo, M.M. Rahman, Biosynthesis of Tithonia diversifolia leaf mediated zinc oxide nanoparticles loaded with flamboyant pods (Delonix regia) for the treatment of methylene blue wastewater, Arab. J. Chem. 14 (2021), 103363.
[13] A.O. Dada, F.A. Adekola, E.O. Odebunmi, A.S. Ogunlaja, O.S. Bello, Two-three parameters isotherm modeling, kinetics with statistical validity, desorption and thermodynamic studies of adsorption of Cu(II) ions onto zerovalent iron nanoparticles, Sci. Rep. 11 (2021), 16454.
[14] B.T. Atunwa, A.O. Dada, A.A. Inyinbor, U. Pal, Synthesis, physiochemical and spectroscopic characterization of palm kernel shell activated carbon doped AgNPs (PKSAC@AgNPs) for adsorption of chloroquine pharmaceutical waste, Mater. Today Proc. (2022).
[15] O.S. Bello, O.C. Alao, T.C. Alagbada, Biosorption of ibuprofen using functionalized bean husks, Sustain. Chem. Pharm. 13 (2019), 100151.
[16] A. Adeolu, O.T. Okareh, A.O. Dada, Adsorption of chromium ion from industrial effluent using activated carbon derived from plantain (Musa paradisiaca) wastes, Am. J. Environ. Protect. 4 (1) (2016) 7–20.
[17] O.A. Ekpete, A.C. Marcus, V. Osi, Preparation and characterization of activated carbon obtained from plantain (Musa paradisiaca) fruit stem, J. Chem. 2017 (2017) 1–6.
[18] E.O. Oyelude, J.A.M. Awudza, S.K. Twumasi, Equilibrium, kinetic and thermodynamic study of removal of eosin yellow from aqueous solution using teak leaf litter powder, Sci. Rep. 7 (2017) 1–10.
[19] K. Ebisike, A.E. Okoronkwo, K.K. Alaneme, Synthesis and characterization of chitosan–silica hybrid aerogel using sol-gel method, J. King Saud Univ. Sci. 32 (2020) 550–554.
[20] O.A. Ekpete, M. Horsfall, Kinetic sorption study of phenol onto activated carbon derived from fluted pumpkin stem waste (*Telfairia occidentalis* Hook. F), ARPN J. Eng. Appl. Sci. 6 (2011) 43–49.
[21] N. Asfaliza Abdullah, P. Sannasi Abdullah, M. Faiz Mohd Amin, N. Azah Zainol, Preparation and characterization of a new biocarbon material derived from Macaranga gigantea (giant 'Mahang') leaf biomass as precursor, Mater. Today Proc. 5 (2018) 21888–21896.
[22] O.S. Bello, B.M. Lasisi, O.J. Adigun, V. Ephraim, Scavenging rhodamine B dye using Moringa oleifera seed pod, Chem. Speciat. Bioavailab. 29 (2017) 120–134.
[23] M. Moyo, L. Chikazaza, B.C. Nyamunda, U. Guyo, Adsorption batch studies on the removal of Pb(II) using maize tassel based activated carbon, J. Chem. 2013 (2013) 1–8, 508934.
[24] A. Leena, T. Santhi, S. Manonmani, Recent developments in preparation of activated carbons by microwave: study of residual errors, Arab. J. Chem. 8 (2015) 343–354.
[25] O.A. Ekpete, M. Horsfall, P. Harcourt, I. Chemistry, P. Harcourt, Preparation and characterization of activated carbon derived from fluted pumpkin stem waste (Telfairia occidentalis Hook F), Res. J. Chem. Sci. 1 (2011) 10–17.
[26] A.O Dada, F.A. Adekola, E.O. Odebunmi, F.E. Dada, O.M. Bello, B.A. Akinyemi, O.S. Bello, O.G. Umukoro, Sustainable and low-cost Ocimum gratissimum for biosorption of indigo carmine dye: kinetics, isotherm, and thermodynamic studies, Int. J. Phytoremediation 22 (14) (2020) 1524–1537.
[27] A.O. Dada, F.A. Adekola, E.O. Odebunmi, A.A. Inyinbor, B.A. Akinyemi, I.D. Adesewa, Kinetics and thermodynamics of adsorption of rhodamine B onto bentonite supported nanoscale zerovalent iron nanocomposite, J. Phys. Conf. Ser. 1299 (2019) 1–10.
[28] C.P. Madu, L. Lajide, Physicochemical characteristics of activated charcoal derived from melon seed husk, J. Chem. Pharmaceut. Res. 5 (2013) 94–98.
[29] O.S. Bello, K.A. Adegoke, O.O. Akinyunni, Preparation and characterization of a novel adsorbent from Moringa oleifera leaf, Appl. Water Sci. 7 (2017) 1295–1305.
[30] O.S. Ayanda, O.S. Fatoki, F.A. Adekola, B.J. Ximba, L.F. Petrik, Kinetics, isotherm and thermodynamics of tributyltin removal by adsorption onto activated carbon, silica and composite material of silica and activated carbon, Desalination Water Treat. 53 (2015) 1361–1370.
[31] M. Hadi, M.R. Samarghandi, G. McKay, Equilibrium two-parameter isotherms of acid dyes sorption by activated carbons: study of residual errors, Chem. Eng. J. 160 (2010) 408–416.
[32] E. Alipanahpour Dil, M. Ghaedi, A. Asfaram, F. Mehrabi, F. Sadeghfar, Efficient adsorption of azure B onto CNTs/Zn:ZnO@Ni2P-NCs from aqueous solution in the presence of ultrasound wave based on multivariate optimization, J. Ind. Eng. Chem. 74 (2019) 55–62.
[33] Y.T. Prabhu, B. Sreedhar, U. Pal, Achieving enhanced photocatalytic activity of ZnO supported on MWCNTs towards degradation of pollutants under visible light, Mater. Today Proc. 8 (2019) 419–426.
[34] H.B. Uma, S. Ananda, M.B. Nandaprakash, High efficient photocatalytic treatment of textile dye and antibacterial activity via electrochemically synthesized Ni-doped ZnO nano photocatalysts, Chem. Data Collect. 24 (2019), 100301.
[35] Y. Dai, Q. Sun, W. Wang, L. Lu, M. Liu, J. Li, S. Yang, Y. Sun, K. Zhang, J. Xu, W. Zheng, Z. Hu, Y. Yang, Y. Gao, Y. Chen, X. Zhang, F. Gao, Y. Zhang, Utilizations of agricultural waste as adsorbent for the removal of contaminants: a review, Chemosphere 211 (2018) 235–253.

[36] S.B. Daffalla, H. Mukhtar, M.S. Shaharun, Preparation and characterization of rice husk adsorbents for phenol removal from aqueous systems, PLoS One 15 (12) (2020), e0243540.
[37] K. Le Van, T.T. Luong Thi, Activated carbon derived from rice husk by NaOH activation and its application in supercapacitor, Prog. Nat. Sci. Mater. Int. 24 (2014) 191–198.
[38] S. Nethaji, A. Sivasamy, A.B. Mandal, Adsorption isotherms, kinetics and mechanism for the adsorption of cationic and anionic dyes onto carbonaceous particles prepared from Juglans regia shell biomass, Int. J. Environ. Sci. Technol. 10 (2013) 231–242.
[39] M.A. Ahmad, N.A. Ahmad Puad, O.S. Bello, Kinetic, equilibrium and thermodynamic studies of synthetic dye removal using pomegranate peel activated carbon prepared by microwave-induced KOH activation, Water Resour. Ind. 6 (2014) 18–35.
[40] S. Wang, Y.-R. Lee, Y. Won, H. Kim, S.-E. Jeong, B. Wook Hwang, A. Ra Cho, J.-Y. Kim, Y. Cheol Park, H. Nam, D.-H. Lee, H. Kim, S.-H. Jo, Development of high-performance adsorbent using KOH-impregnated rice husk-based activated carbon for indoor CO_2 adsorption, Chem. Eng. J. 437 (2022), 135378.
[41] Rinawati, D. Hidayat, R. Supriyanto, D.F. Permana, Yunita, Adsorption of polycyclic aromatic hydrocarbons using low-cost activated carbon derived from rice husk, J. Phys. Conf. Ser. 1338 (2019).
[42] C. Saka, BET, TG-DTG, FT-IR, SEM, iodine number analysis and preparation of activated carbon from acorn shell by chemical activation with ZnCl2, J. Anal. Appl. Pyrolysis 95 (2012) 21–24.